In situ monitoring of lepidocrocite bio-reduction and magnetite formation by reflexion Mössbauer spectroscopy

REVISION 2

Asfaw Zegeye*, Mustapha Abdelmoula, Muhammad Usman, Khalil Hanna, Christian Ruby

Laboratoire de Chimie Physique et Microbiologie pour l'Environnement, LCPME, UMR 7564, Institut Jean Barriol, CNRS-Nancy Université, 405 rue de Vandoeuvre, 54600, Villers-lès-Nancy, France.

***** *Corresponding Author*: Asfaw.zegeye@lcpme.cnrs-nancy.fr

ABSTRACT

The miniaturized Mössbauer spectrometer (MIMOS II) was used to monitor *in situ* the mineralogical transformation of lepidocrocite (γ-FeOOH) in a *Shewanella putrefaciens* culture under anaerobic conditions using methanoate as the electron source. Magnetite was the only biogenic mineral formed during the course of the incubation. The analysis of the biogenic mineral by transmission electron microscopy (TEM) revealed cubic-shaped crystals with a relatively homogeneous grain size of about 50 nm. After one day of incubation, the departure from stoichiometry, δ, of the biogenerated magnetite was very low (δ ~ 0.025) and rapidly reached values close to zero. Such low values of δ were not obtained for magnetite synthesized inorganically when Fe^{3+} in the form of γ-FeOOH was reacted with stoichiometric quantities of soluble Fe^{2+} and OH^-. The experimental setup used in this study could be replicated in field experiments when assessing the formation of magnetite in modern geological settings as its formation is suspected to be caused by a strong bacterial activity.

Keywords: MIMOS, magnetite, stoichiometry, biomineralisation

INTRODUCTION

Magnetite, a mixed valence Fe(II-III) oxide ($Fe_{3-\delta}O_4$), is a commonly occurring mineral on Earth usually found in soils and sediments (Cornell and Schwertmann 1996). Under non-sulfidic reducing conditions, dissimilatory iron-reducing bacteria (DIRB) can play an important role in the biogeochemistry of iron by coupling the oxidation of an electron source (organic matter or H_2) to the external reduction of iron oxyhydroxides (Nealson and Saffarini 1994). Thus, Dos Santos and Stumm (1992) and Lovley et al. (1991) suggested that most of the Fe(III) reduction occurring in such environments is due to bacterial activity. Depending on the geochemical environments in which Fe(III) bio-reduction takes place, DIRB activity can lead to diverse biogenic minerals such as magnetite, the discovery of which at a depth of 6.7 km below the surface has been used as a marker for DIRB activity (Gold 1992; Lovley et al. 1987). Moreover, the quantity of DIRB-induced extracellular magnetite per unit of biomass could be several thousand times more than magnetite formed by magnetotactic bacteria (Frankel 1987; Lovley 1991). Whereas many reports have focused on magnetite precipitated by magnetotactic bacteria (Kim et al. 2005; Kopp and Kirschvink 2008), very few reports (Gibbs-Eggar et al. 1999) have been able to demonstrate the unequivocal existence of extracellularly precipitated magnetite. This could be explained by the higher reactivity of magnetite formed by DIRB leading to the paucity of magnetite in the natural environment (Kukkadapu et al. 2005; Li et al. 2009). Indeed, the reactivity and stability of magnetite is dictated partly by its stoichiometry defined by $x = Fe^{3+} / \{Fe^{2+} + Fe^{3+}\}$ where $0.67 \leq x \leq 1$, with stoichiometric magnetite ($x = 0.67$ or $\delta = 0$) being the most reactive composition (Cutting et al. 2010; Gorski and Scherer 2009). It was shown that stoichiometric magnetite had a lower reduction potential than that of non-stoichiometric magnetite, consistent with higher reactivity toward pollutants such as nitrobenzene compounds (Gorski et al. 2010).

Numerous laboratory studies have pointed out that geochemical parameters such as the nature of the iron oxide, the concentration of dissolved Fe^{2+}, the bacteria/iron oxide ratio, and the physiochemical characteristics of the culture media could have an impact on the subsequent mineralization of magnetite (Fredrickson et al. 1998; Roh et al. 2003; Zachara et al. 1998; Zegeye et al. 2010). These studies mainly focused on gaining a better understanding of the bio-reduction processes by characterizing the secondary mineral. While the stoichiometry of the magnetite as a secondary mineral has widely been investigated at the end of the bio-reduction reaction (Kukkadapu et al. 2005; Li et al. 2009), the evolution of the stoichiometry of magnetite during its formation has not yet been fully studied. Indeed, to understand the stability of a biogenic magnetite and its persistence in soils and sediments a thorough investigation of the evolution of its stoichiometry during bio-reduction is needed.

EXPERIMENTAL METHODS

Bioreduction Experiments:

In order to investigate the fluctuation of magnetite stoichiometry during iron bio-reduction, we examined microbially induced lepidocrocite reduction using *Shewanella putrefaciens* CIP 8040, a facultative DIRB. The lepidocrocite was prepared by aerobic oxidation of $FeCl_2$ in sodium hydroxide solution (Schwertmann and Cornell 2000). An anaerobic cell suspension (10^6 CFU mL^{-1}) was used to inoculate a non-growth-supporting medium containing sodium methanoate (1 mM) as the electron source and lepidocrocite (3 mM) as the electron acceptor under strict anaerobic conditions as described in a recent study (Zegeye et al. 2007). The control experiment was cell-free and otherwise identical to the biotic sample.

Reflexion Mössbauer Spectroscopy and Transmission Electron Microscopy (TEM):

The precipitation of biogenic magnetite was monitored *in situ* by using a miniaturized Mössbauer spectrometer (MIMOS), designed for Mars missions (Klingelhoefer et al. 2003),

and adapted to laboratory measurements (Fig. 1, complementary data). The MIMOS works in back-scattering geometry, without sample preparation and/or thickness matrix effect correction, and thereby differs from transmission Mössbauer spectroscopy. Re-emitted backscattered γ-rays (14.4 keV) were selected by four Si-PIN-diodes detectors. Centre shifts *CS* were reported with respect to that of α-Fe at room temperature. Mössbauer spectra were computer-fitted (recoil software, Ottawa University) with a sum of Lorentzian shape lines, which excludes a particle size distribution model. The relative areas of iron fitted in different sites have not been calibrated by the recoilless fraction, due to its relatively small contribution (Eeckhout and De Grave 2003; Sawatzky et al. 1969).

TEM observations and selected area electron diffraction (SAED) were carried out using a Philips CM20 TEM (200 kV) at the end of the incubation period (*i.e.* 26 days). One drop of the suspension was laid on an amorphous-carbon-coated grid and loaded into the analysis holder of the microscope under 10^{-8} Torr vacuum.

RESULT AND DISCUSSION

The lepidocrocite and magnetite spectra displayed a doublet and two sextets respectively (Figure 1) with Mössbauer hyperfine parameters (Table 1, complementary data) similar to those published in the literature (Da Costa et al. 1998; De Grave et al. 2002). For stoichiometric magnetite, Fe_3O_4, the outer sextet, S_A, corresponds to $^{Tet}Fe^{3+}$ ions in the tetrahedral A-sites, whereas the inner sextet S_B corresponds to the $^{Oct}Fe^{2+}$ and the $^{Oct}Fe^{3+}$ ions present in the octahedral B-sites. In fact, due to very fast electron hopping between the $^{Oct}Fe^{2+}$ and the $^{Oct}Fe^{3+}$ ions at temperatures above the Verwey transition (121 K), the sextet S_B observed by Mössbauer spectroscopy is integrated into a peak representing an average valence of $^{Oct}Fe^{2.5+}$ ions. The analysis of Mössbauer spectra showed that magnetite precipitated as the only biogenic mineral and indicated that 6 % of the initial lepidocrocite remained at the end of the incubation period (Figure 1f, d = 26). During magnetite formation,

no intermediate mineral, such as green rust, was observed, which indicates that the solution was supersaturated with respect to magnetite (Figure 1). In contrast, no lepidocrocite transformation was detected at any time during the control experiment (data not shown), thereby indicating that the MIMOS can be used to assess mineralogical transformation ensuing from bacterial activity.

TEM images of the secondary mineral revealed aggregates of magnetite crystals with only slight differences in size and morphology (Figure 2a). The particles consisted of cubic-shaped crystals with a relatively homogeneous grain size of ~ 50 nm. The grain size measured in this study was in the upper range of the usual grain size observed for bio-induced magnetite (10-120 nm) and therefore would not display superparamagnetism (Li et al. 2009; Vali et al. 2004). The *d*-spacings calculated from SAED (Table 2, complementary data) were characteristic of magnetite and confirmed its presence as the sole secondary mineral (Figure 2b).

An interesting observation in this study was the evolution of magnetite stoichiometry during the bio-reduction process. The general formula of magnetite is $^{Tet}Fe^{3+}[^{Oct}Fe^{2+}_{(1-3\delta)}Fe^{3+}_{(1+2\delta)}V_{\delta}]O_4$, ($0 \leq \delta \leq 1/3$), where "V" denotes the cations vacancies accounting for charge balance. For non-stoichiometric magnetite ($0 < \delta \leq 1/3$), a first fraction of the $^{Oct}Fe^{3+}$ species participates in the electron hopping and a second fraction screens the lack of charge of the cations vacancy (Coey et al. 1971; Ramdani et al. 1987; Voogt et al. 1999). In order to distinguish between the two $^{Oct}Fe^{3+}$ species, the formula of non-stoichiometric magnetite can be rewritten as $^{Tet}Fe^{3+}[^{Oct}\{Fe^{2+}_{(1-3\delta)}Fe^{3+}_{(1-3\delta)}\}Fe^{3+}_{5\delta}V_{\delta}]O_4$. The Mössbauer spectrum of $Fe_{3-\delta}O_4$ at room temperature consists of three sextets: (1) S_{B1} corresponding to the $^{Oct}Fe^{2.5+}$ ions, (2) S_{B2} associated to the $^{Oct}Fe^{3+}$, (3) S_A corresponding to the $^{Tet}Fe^{3+}$ ions (Vandenberghe et al. 2000). However, the hyperfine parameters of sextets S_A and S_{B2} are very close to each other and the spectrum of a non-stoichiometric magnetite can

126 be fitted with only two sextets (Gorski and Scherer 2010; Voogt et al. 1999), the outer sextet
127 corresponding to the superposition of sextets S_A and S_{B2} and the inner sextet representing S_{B1}.
128 The ratio between the relative area (*RA*) of the sextets $\beta = RA\ (S_A + S_{B2}) / RA\ (S_{B1})$ is therefore
129 $(1+5\delta) / (2-6\delta)$ and the vacancy degree can be deduced as $\delta = (2\beta - 1) / (6\beta + 5)$. From the
130 experimental values of β, the vacancy parameter δ of magnetite was calculated as a function
131 of the incubation time (Figure 3). The initial magnetite formed after one day of incubation has
132 a very slight departure from stoichiometry $\delta \sim 0.025$, and a value very close to $\delta \sim 0$ was
133 reached after 5 days. After 7 days, a magnetite with an apparent excess of Fe^{2+} corresponding
134 to a negative value $\delta \sim -0.02 \pm 0.01$ was measured. Despite the fact that biogenic magnetite
135 that were precipitated in *Shewanella* cultures and contained a slight excess of Fe^{2+} ions in
136 their structure have already been reported in previous research (Kukkadapu et al. 2005; Li et
137 al. 2009), the negative departure from stoichiometry measured in this study was very close to
138 the experimental error. It is therefore difficult to unambiguously conclude that a negative
139 value of δ would be characteristic of a transient state of magnetite during the bioreduction
140 process. Finally, the product obtained after 26 days of incubation was a stoichiometric
141 magnetite Fe_3O_4. For comparison, an abiotic experiment was conducted by adding soluble
142 Fe^{2+} ions to a suspension of lepidocrocite at a fixed value of the ferric molar fraction $x = 0.67$
143 to form a stoichiometric magnetite according to the following reaction:

144 $$2\ \gamma\text{-}Fe^{III}OOH + Fe^{2+} + 2\ OH^- = Fe^{II}Fe^{III}{}_2O_4 + 2\ H_2O \quad (1)$$

145 The precipitation of magnetite was achieved by adding to this initial suspension a basic
146 solution of NaOH with an OH^-/Fe^{3+} molar ratio of 1. The suspension was agitated for an hour
147 and aged in a static condition for 26 days. The vacancy parameter of this abiotic magnetite
148 was measured for three aging times, *i.e.* 1 hour, 1 day, and 26 days (Fig. 3) by recording the
149 corresponding Mössbauer spectra. About 75 % of the lepidocrocite was transformed into a
150 quasi-stoichiometric magnetite after 1 hour of aging. After both 1 day and 26 days of aging

time, the rest of lepidocrocite was transformed into a magnetite with a vacancy parameter close to $\delta \sim 0.05$.

The Fe(II)-Fe(III) mass-balance diagram previously described by Ruby et al. (2006) presents the domain of composition $x = Fe^{3+} / [Fe^{2+} + Fe^{3+}]$ corresponding to the vacancy parameter δ of the biotic and abiotic magnetite synthesized in this study ($x = \{2+2\delta\}/\{3-\delta\}$). The value of x for each incubation time is determined by the following formula:

$$x = RA\ (\gamma\text{-FeOOH}) + RA\ (Fe_{3-\delta}O_4)\ \{2+2\delta\}/\{3-\delta\}, \quad (2)$$

where RA (γ-FeOOH) and RA ($Fe_{3-\delta}O_4$) are the relative areas of the lepidocrocite and magnetite components of the Mössbauer spectra (Table 1, complementary data), respectively. The values of x for several incubation times are presented at the bottom right of Figure 4. It decreases gradually between $x = 0.84$ and $x = 0.68$ for incubation times varying between 1 day and 26 days, respectively. The composition of the suspension is, therefore, favorable to the formation of a magnetite having relatively high departure from the stoichiometric value $x = 0.67$. However, in both experiments, the departure from stoichiometry was relatively limited if it is compared to the global domain of composition of magnetite, a solid solution that is bounded by $x = 0.67$ for Fe_3O_4 and $x = 1$ for maghemite γ-Fe_2O_3. Nevertheless, magnetite was formed with a composition very close to $^{Tet}Fe^{3+}[^{Oct}Fe^{2+}Fe^{3+}]O_4$ ($\sim 0.65 \leq x \leq \sim 0.69$) during the entirety of the bioreduction experiment. Because DIRB reduce the Fe (III) oxide into Fe^{2+} in a progressive manner, one would expect that x would decrease gradually from $x = 1$ to $x = 0.67$. However, the local biological conditions favor the formation of a mixture of lepidocrocite and stoichiometric magnetite rather than a non-stoichiometric magnetite, which would become stoichiometric during the course of the reduction along the reaction path A_1B (Fig. 4). Such a stoichiometric magnetite was not obtained during the abiotic experiment despite the fact that stoichiometric conditions were imposed. Reaction (1) corresponding to the segment A_2B was, therefore, not fully accomplished and a small part of

176 the soluble Fe(II) ions which was present in the initial solution did not incorporate in the final
177 solid product, i.e. $Fe_{2.95}O_4$, leading to a non-stoichiometric magnetite. Similarly, Gorski and
178 Scherer (2009, 2010) pointed out that excessive washing of a stoichiometric magnetite caused
179 the magnetite to become oxidized due to Fe^{2+} dissolution. We, therefore, speculate that an
180 excess of Fe^{2+} (more than what is needed for stoichiometric magnetite) in the synthesis
181 solution is needed to maintain the stoichiometry of the abiotic magnetite. On the other hand,
182 DIRB were able to maintain a flux of Fe^{2+} to sustain the stoichiometry of the biogenic
183 magnetite.

184 To our knowledge this is the first study reporting the *in situ* monitoring of a biogenic
185 magnetite ($Fe_{3-\delta}O_4$) stoichiometry during its formation. The relative proportion of the two
186 sextets S_A and S_B of the Mössbauer spectrum of the magnetite were used to determine the
187 eventual departure from stoichiometry δ. The resulting magnetite was stoichiometric with
188 $\delta = 0$. The paucity of bacterially induced magnetite in the environment could be explained by
189 their reactivity which is related to their stoichiometry. Recently, the MIMOS apparatus was
190 used to study *in situ* the mineralogical transformation of Fe-containing compounds in
191 hydromorphic soils (Feder et al., 2005). Therefore, the experimental approach used in the
192 present study could be applied in field experiments to assess *in situ* the formation of biogenic
193 magnetite in modern geological settings where its formation is suspected to be caused by a
194 strong bacterial activity.

195

196 **ACKNOWLEDGMENTS**

197

198 The authors would like to thank the Agence Nationale de la Recherche (ANR) and Agence de
199 la Maîtrise de l'Energie (ADEME) for financial support (programme Ecotech 2009,
200 CERVEAU NP, décision attributive d'aide n° 0994C0103). We would like to thank the

201 Lorraine Region for financing of the MIMOS apparatus (CPER 2005-2009). The authors
202 acknowledge J. Ghanbaja (Nancy Université) for the TEM analyses.
203

REFERENCES

Coey, J.M.D., Morrish, A.H., and Sawatzky, G.A. (1971) Mössbauer study of conduction in magnetite. Journal de Physique, C1-271-C1-273.

Cornell, R.M. and Schwertmann, U. (1996) The iron oxides: structure, properties, reactions, occurrences and uses. 573 pages p. VCH, Weinheim, Germany.

Cutting, R.S., Coker, S.V., Telling, N.D., Kimber, R.L., Pearce, C.I., Ellis, B.L., Lawson, R.S., van Der Laan, G., Pattrick, R.A.D., Vaughan, D.J., Arenholz, E., and Lloyd, J.R. (2010) Optimizing Cr(VI) and TC(VII) remediation through nanoscale biomineral engineering. Environmental Science and Technology, 44, 2577-2584.

Da Costa, G.M., De Grave, E., and Vanderberghe, R.E. (1998) Mössbauer studies of magnetite and Al-substituted maghemites. Hyperfine Interaction, 117, 207-243.

De Grave, E., Barrero, C.A., Da Costa, G.M., Vanderberghe, R.E., and Van San, E. (2002) Mössbauer spectra α- and γ- polymorphs of FeOOH and Fe_2O_3: effects of poor crystallinity and of Al-for-Fe substitution. Clay Minerals, 37, 591-606.

Dos Santos, A.M. and Stumm, W. (1992) Reductive dissolution of iron (III) (hydr)oxides by hydrogen sulfide. Langmuir, 8, 1671-1675.

Eeckhout, S.G. and De Grave, E. (2003) Evaluation of ferrous and ferric Mössbauer fractions. Part II. Physics and Chemistry of Minerals, 30, 142-146.

Feder, F., Trolard, F., Klingelhöfer, G. and Bourrié, G. (2005) In situ Mössbauer spectroscopy: evidence for green rust (fougerite) in a gleysol and its transformation with time and depth. Geochimica et Cosmochimica Acta, 69, 4463-4483.

Frankel, R.B. (1987) Anaerobes pumping iron. Nature, 330, 208-208.

Fredrickson, J.K., Zachara, J.M., Kennedy, D.W., Dong, H., Onstott, T.C., Hinman, N.W., and Li, S.-M. (1998) Biogenic iron mineralization accompanying the dissimilatory reduction of hydrous ferric oxide by a groundwater bacterium. Geochimica et Cosmochimica Acta, 62, 3239-3257.

Gibbs-Eggar, Z., Jude, B., Dominik, J., Loiseau, J.L., and Oldfield, F. (1999) Possible evidence for dissimilatrory bacterial magnetite dominating the magnetite properties of recent lake sediments. Earth and Planetary Science Letters, 168, 1-6.

Gold, T. (1992) The deep, hot biosphere. Proceedings of the National Academy of Science, 89, 6045-6049.

Gorski, C. and Scherer, M.M. (2009) Influence of magnetite stoichiometry on Fe^{II} uptake and nitrobenzene reduction. Environmental Science and Technology, 43, 3675-3680.

Gorski, C. and Scherer, M.M. (2010) Determination of nanoparticulate magnetite stoichiometry by Mössbauer spectroscopy, acidic dissolution, and powder X-ray diffraction: A critical review. American Mineralogist, 95, 1017-1026.

Gorski, C., Nurmi, J.T., Tratnyek, P.G., Hofstetter, B., and Scherer, M.M. (2010) Redox behaviour of magnetite: implication for contaminant reduction. Environmental Science and Technology, 44, 55-60.

Kim, D.K., Kodama, K.P., and Moeller, R.E. (2005) Bacterial magnetite produced in water column dominates lake sediment mineral magnetism: Lake Ely, USA. Geophysical Journal International, 163, 26-37.

Klingelhoefer, G., Morris, R.V., Bernhardt, B., Rodionov, D., De Souza, P.A., Squyres, S.W., Foh, J., Kankeleit, E., Bonnes, U., Geller, R., Schroeder, C., Linkin, S., Evlanov, E., Zubkov, B., and Prilutski, O. (2003) Athena MIMOS II Mössbauer spectrometer investigation. Journal of Geophysical Research, E12, 108.

Kopp, R.E., and Kirschvink, J.L. (2008) The identification and biogeochemical interpretation of fossil magnetotactic bacteria. Earth Science Review, 86, 42-61.

Kukkadapu, R.K., Zachara, J.M., Fredrickson, J.K., Kennedy, D.W., Dohnalkova, A.C., and McCready, D.E. (2005) Ferrous hydroxycarbonate is a stable transformation product of biogenic magnetite. American Mineralogist, 90, 510-515.

Li, Y.L., M., P.S., Dyar, M.D., Vali, H., Konhauser, K., Cole, D.R., Rondinone, A.J., and Phelps, T.J. (2009) Degeneration of biogenic superparamagnetic magnetite. Geobiology, 7, 25-34.

Lovley, D.R. (1991) Magnetite formation during microbial iron reduction. In R.B. Frankel, and R.P. Blakemore, Eds. Iron biominerals, p. 155-166. Plenum, New York, NY.

Lovley, D.R., Stolz, J.F., Nord, G.L., and Phillips, E.J.P. (1987) Anaerobic production of magnetite by a dissimilatory iron-reducing microrganism. Nature, 330, 252-54.

Lovley, D.R., Phillips, E.J.P., and Lonergan, D.J. (1991) Enzymatic versus nonenzymatic mechanisms for Fe(III) reduction in aquatic sediments. Environmental Science and Technology, 25, 1062-1067.

Nealson, K.H. and Saffarini, D. (1994) Iron and manganese in anaerobic respiration: environmental significance, physiology, and regulation. Annual Review of Microbiology, 48, 311-43.

Ramdani, A., Steinmetz, J., Gleitzer, C., Coey, J.M.D., Friedt, J.M. (1987) Perturbation de l'échange électronique rapide par les lacunes cationiques dans $Fe_{3-x}O_4$ ($x<0,09$). Journal of Physics and Chemistry of Solids, 48, 217-228.

Roh, Y., Zhang, C.L., Vali, H., Lauf, R.J., Zhou, J., and Phelps, T.J. (2003) Biogeochemical and environmental factors in Fe biomineraliztion: magnetite and siderite formation. Clays and Clay Minerals, 51, 83-95.

Ruby, C., Rabha, A., Gehin, A., Cortot, J., Abdelmoula, M., and Genin, J.M. (2006) Green rusts synthesis by coprecipitation of Fe^{II}-Fe^{III} ions and mass balance diagram. Comptes Rendus Geosciences, 338, 420-432.

Schwertmann, U. and Cornell, R.M. (2000) Iron oxide in the laboratory: Preparation and characterization. Wiley-VCH, New York.

Sawatzky, G. A., Van der Woude, F., and Morrish, A. H. (1969) Recoiless-fraction ratios for Fe^{57} in octahedral and tetrahedral sites of a spinel and a garnet. Physics Reviews, 183, 383-386.

Vali, H., Kleiss, B., Li, Y.-L., Sears, S.K., Kim, S.S., Kirschvink, L., and Zang, C.L. (2004) Formation of tabular single-domain magnetite induced by geobacter metallireducens GS-15. Proceedings of the National Academy of Science, 10, 16121-16126.

Vandenberghe, R.E., Barrero, C.A., Da Costa, G.M., Van San, E., and De Grave, E. (2000) Mössbauer characterization of iron oxides and (oxy)hydroxides: the present state of the art. Hyperfine Interactions, 126, 247-259.

Voogt, T., Fujii, T., Smulders, P.J.M., Niesen, L., A., J.M., and Hibma, T. (1999) NO_2-assissted molecular beam epitaxy of Fe_3O_4, $Fe_{3-\delta}O_4$, and γ-Fe_2O_3 thin films on MgO (100). Physical Review B: Condensed Matter and Materials Physics, 60, 11193-11206.

Zachara, J.M., Li, S.-M., Kennedy, D.W., Smith, S.C., and Gassman, P.L. (1998) Bacterial reduction of crystalline Fe^{3+} oxides in single phase suspensions and subsurface materials. American Mineralogist, 83, 1426-43.

Zegeye, A., Ruby, C., and Jorand, F. (2007) Kinetic and thermodynamic analysis during dissimilatory γ-FeOOH reduction: formation of green rust 1 and magnetite. Geomicrobiology Journal, 24, 51-64.

Zegeye, A., Mustin, C., and Jorand, F. (2010) Bacterial and iron aggregates mediate secondary iron mineral formation: green rust versus magnetite. Geobiology, 8, 209-222.

Figures captions:

Figure 1: Mössbauer spectra of solid compounds obtained at different incubation times. (a) Initial mineral, (b) 1 day, (c) 2 days, (d) 5 days, (e) 9 days, and 26 days. The hyperfine parameters collected at room temperature are shown in Table 1 (complementary data).

Figure 2: (a) TEM image of mineral formed after 26 days of incubation whose structure is determinate by the SAED analysis (b).

Figure 3: Vacancy parameter δ of magnetite calculated as a function of the incubation time. (■) biogenic magnetite, (▲) abiotic magnetite

Figure 4: Fe^{2+}-Fe^{3+} mass balance diagram showing the composition domain of biotic and abiotic magnetite and the ferric molar fraction *x* of the suspension at different incubation time (right bottom)

Supplementary data, Figure, Tables captions:

Table 1: Mössbauer hyperfine parameters of microbially formed magnetite during lepidocrocite reduction for different times of incubation. Errors on center shift and (CS) quadrupole splitting (Δ) were estimated at ± 0.02mm/s. The error on the internal magnetic filled was ± 5kOe (H) and 2% for the relative abundance (RA). ε corresponds to the quadrupole shift.

Table 2: d_{hkl} parameters of magnetite calculated from selected area electron diffraction (SAED) analysis from the present study and compared to literature data. *(Cornell and Schwertmann 1996)

Figure 1: Experimental setup: The MIMOS is a miniaturized Mössbauer spectrometer and the anaerobic incubation cell sample is in contact with the instrument. MIMOS instrument operate in back scattering geometry. A Co^{57} source irradiates a sample area 10 mm from the detector surface. The Resonant emission and absorption of γ-rays coming from the sample crosses a mylar window placed on the incubation cell.

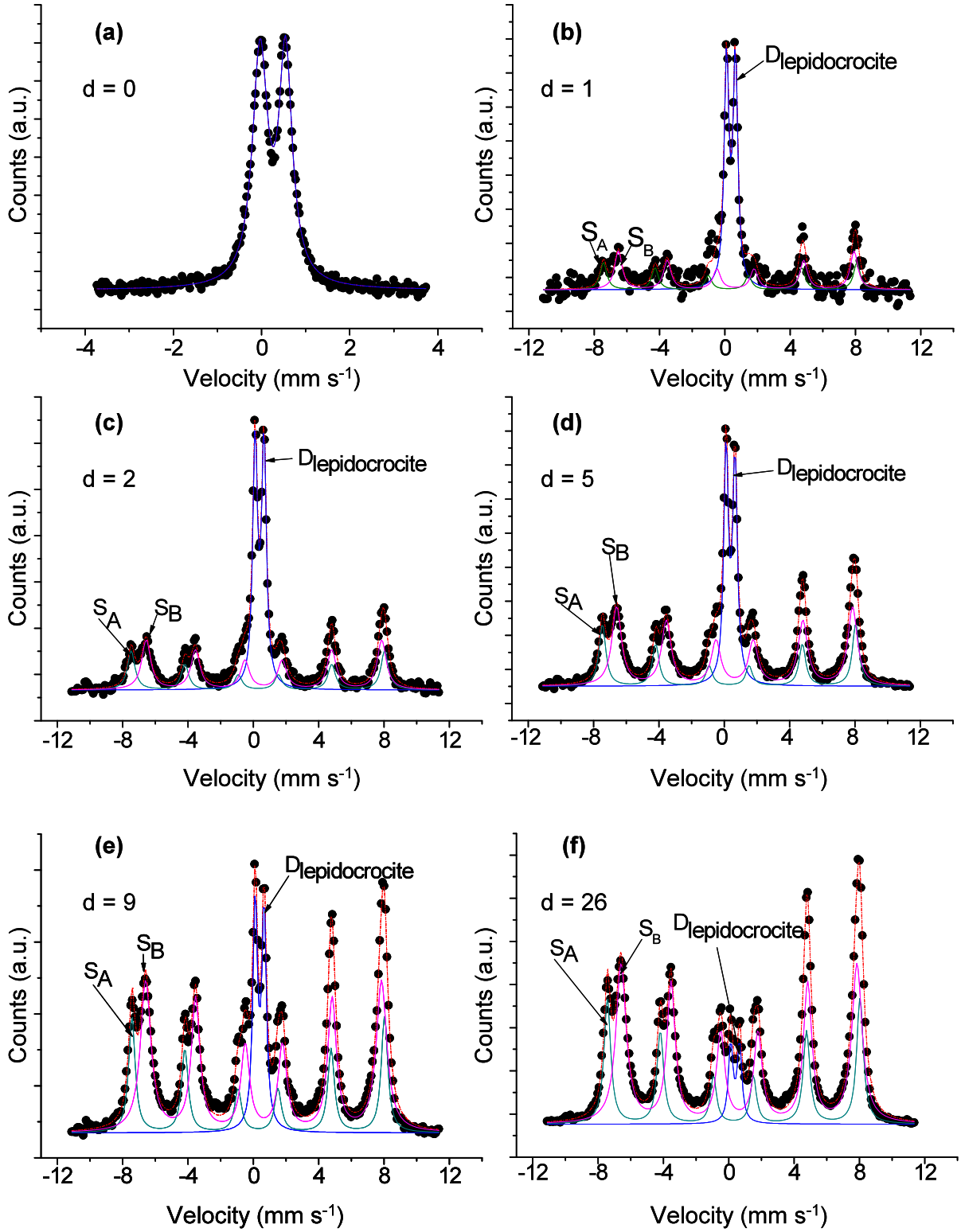
(a)
d = 0
(b)
d = 1
$D_{lepidocrocite}$
S_A
S_B
(c)
d = 2
(d)
d = 5
(e)
d = 9
(f)
d = 26
Counts (a.u.)
Velocity (mm s^{-1})

Figure 1

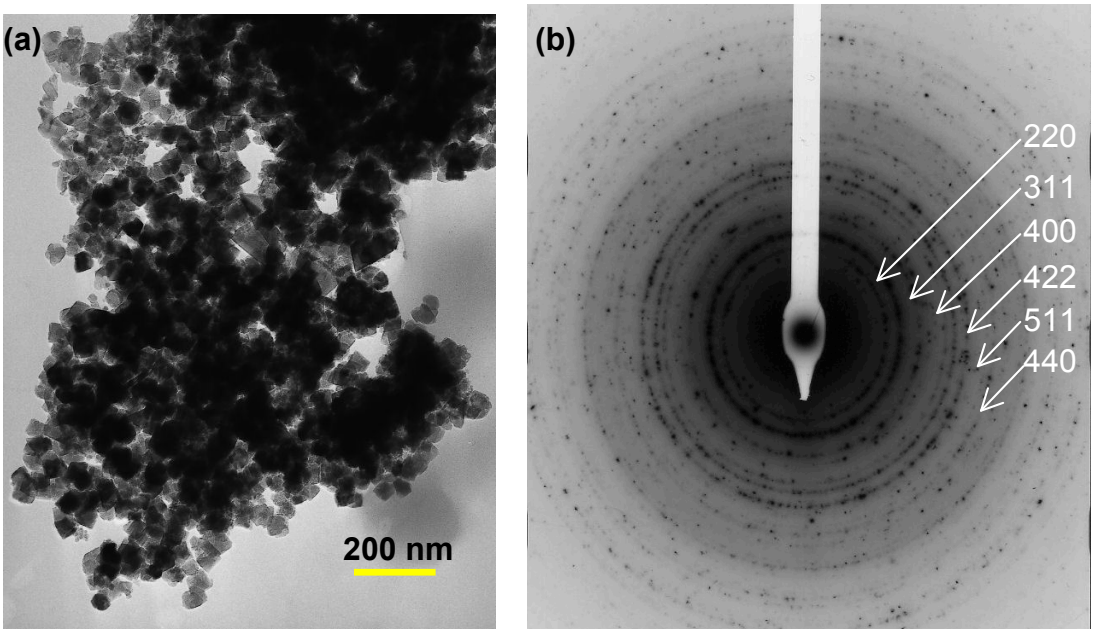

Figure 2

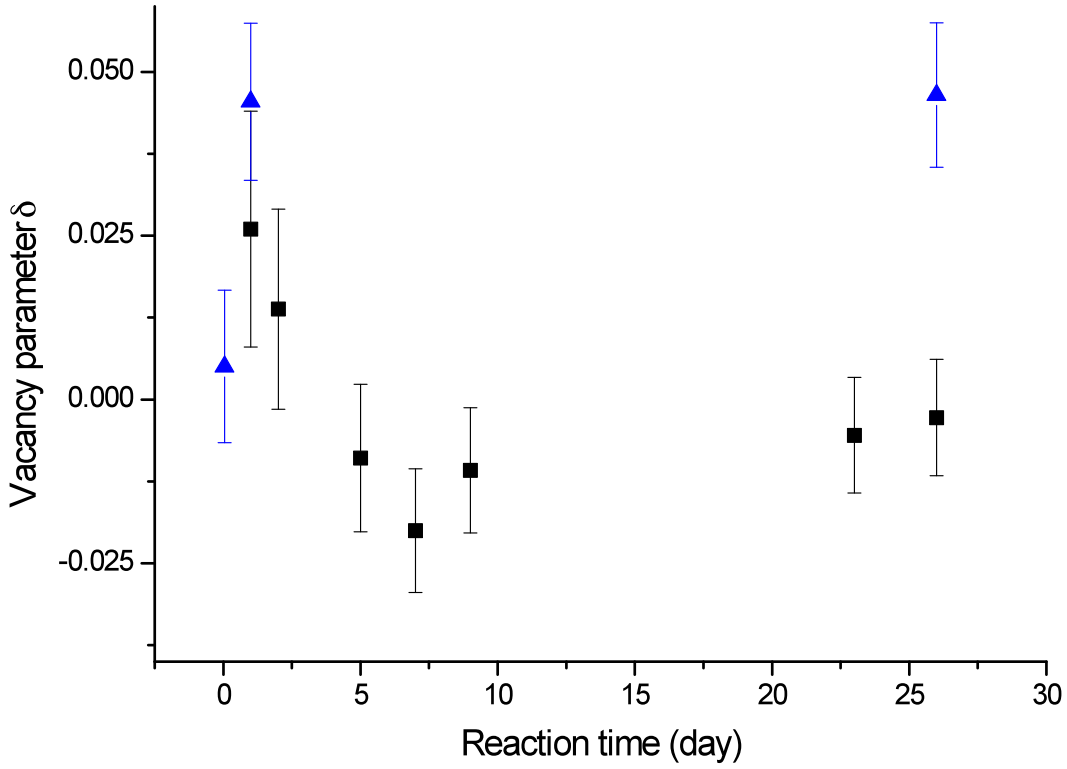
0.050
0.025
0.000
-0.025
Vacancy parameter δ
0
5
10
15
20
25
30
Reaction time (day)

Figure 3

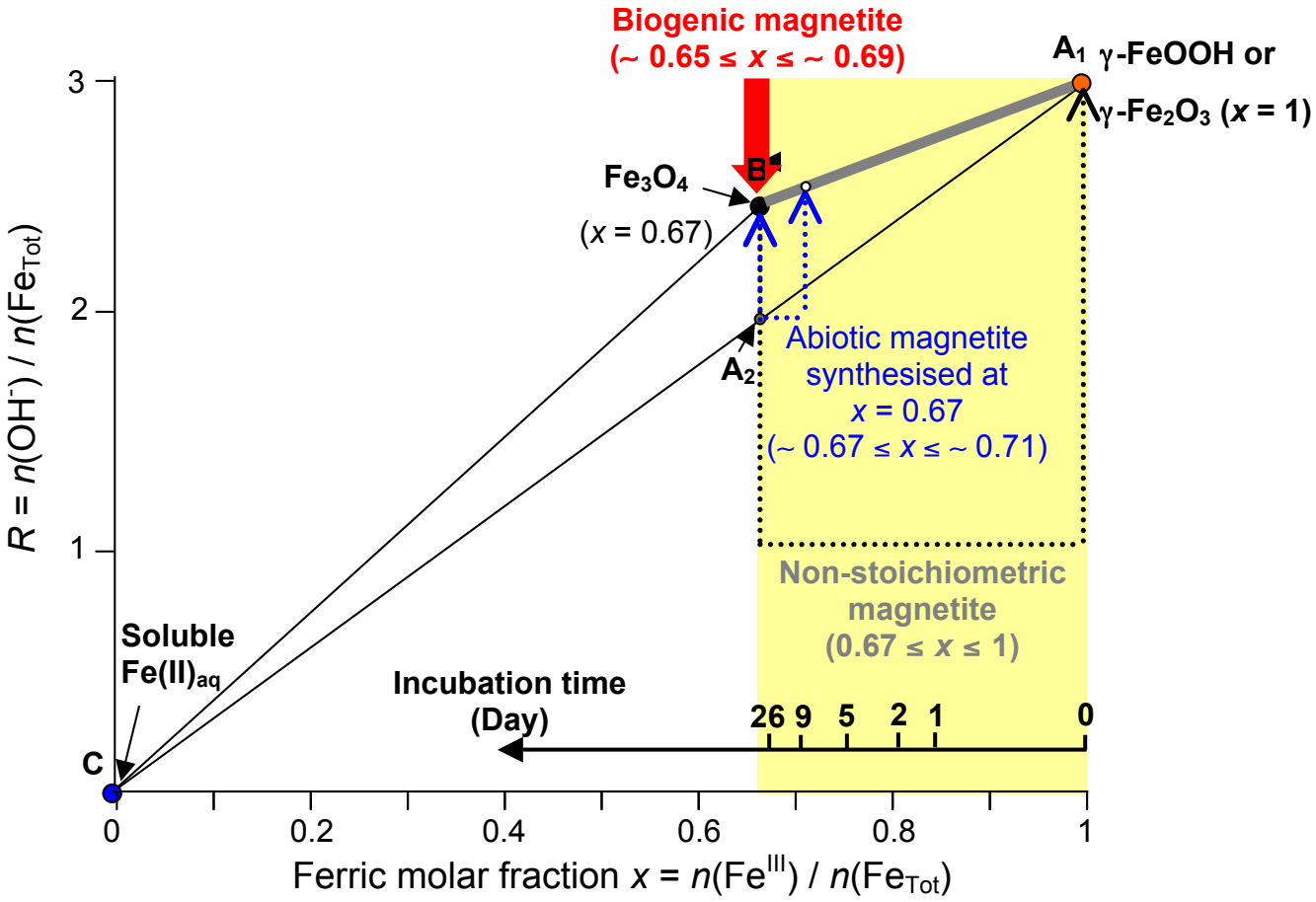
Biogenic magnetite
(~ 0.65 ≤ x ≤ ~ 0.69)
A1 γ-FeOOH or
γ-Fe2O3 (x = 1)
Fe3O4
(x = 0.67)
B
A2
Abiotic magnetite
synthesised at
x = 0.67
(~ 0.67 ≤ x ≤ ~ 0.71)
Non-stoichiometric
magnetite
(0.67 ≤ x ≤ 1)
Soluble
Fe(II)aq
C
Incubation time
(Day)
26 9 5 2 1 0
R = n(OH-) / n(FeTot)
Ferric molar fraction x = n(FeIII) / n(FeTot)
0
0.2
0.4
0.6
0.8
1
1
2
3

Figure 4